Front. Energy Power Eng. China 2009, 3(1): 109–116
DOI 10.1007/s11708-009-0003-3

RESEARCH ARTICLE

Chaokui QIN, Hongmei LU, Xiong LIU, Gerhard SCHMITZ

Engine-driven hybrid air-conditioning system

Abstract A hybrid air-conditioning system that combines an engine-driven chiller with desiccant dehumidification was configured and experimentally tested to provide reliable data for energy consumption and operation cost. The engine performance and the desiccant wheel performance were measured and a numeric model previously set up for dehumidification capacity prediction was validated. For a reference building, the results based upon measured data show that under present electricity/gas price ratio, more than 40% of operation cost can be saved by the hybrid system.

Keywords engine-driven chiller, desiccant wheel, hybrid air-conditioning system, energy consumption

1 Introduction

Maclaine-Cross proposed an engine-driven hybrid air-conditioning system (EDHAS) configuration in 1988 [1], in which an engine-driven chiller combined with an electric chiller accommodated a hotel. A packaged air handling unit (AHU), which mainly consisted of a desiccant wheel and a sensible heat exchanger (HX), powered by reclaimed heat from a gas-engine, provided fresh air. The initiative of his EDHAS proposal was to decrease peak electricity by transferring latent load to waste heat at a reasonable price. Later, Parsons and Pesaran [2] explored the possibility of reclaiming waste heat from gas heat pump (GHP) to supplement heating in winter, and to enhance cooling in summer. Their calculations showed that in most climate regions in the US, such a hybrid system could defeat electric AC systems. From then on, many proposals [3,4] that combined engine-driven chiller or heat pump with desiccant dehumidification have been researched.

Desiccant wheel can fulfill dehumidification task by heat/mass transfer because desiccant is a special kind of hygroscopic material which has a strong affinity for vapor. While in conventional AC systems, the air must be deeply cooled below dew point to make vapor condense. Afterwards, the deeply cooled air has to be reheated to a comfortable temperature before delivery. Although this process, first deeply cooled and then reheated, wastes a lot of energy for dehumidification, yet it has been adopted by designers for a long time due to its simplicity and ease of control. If desiccant dehumidification is incorporated, this energy-consuming thermodynamic process can be avoided, which will bring some inherent advantages. For example, the humidity control independent of temperature can be realized; fan coils (FC) distributed in AC rooms can work under "dry" conditions, preventing fungus growth and therefore improving indoor air quality (IAQ); and, with latent load being undertaken by the desiccant, chilled water of higher temperature (or natural cooling source) can be used for sensible cooling.

The climate in Shanghai and southern areas of China is hot with abnormally high humidity. The design condition of ambient air in Shanghai is 34°C and 65%RH. The consumption of treating fresh air usually accounts for 1/3 of AC system energy consumption. Under such climate conditions, the findings of previous researches are not applicable if no adaptation is made, because the maximum dehumidification capacity of available desiccant equipment at present is limited to about 8 g/kg. Qin and Liu [5] proposed two different EDHAS systems to accommodate the high humidity. One incorporated pre-cooling with an engine-driven chiller, while the other combined desiccant dehumidification with passive dehumidification (enthalpy exchange). The initiatives of these approaches were to

Received June 12, 2008; accepted August 25, 2008

Chaokui QIN, Hongmei LU (✉), Xiong LIU
Mechanical Engineering School, Tongji University, Shanghai 201804, China
E-mail: nehzlu@163.com

Gerhard SCHMITZ
Technical University Hamburg-Harburg, Hamburg 21073, Germany

explore the potential benefits of the hybrid system compared with conventional systems.

Whether the increasing complexity of the proposed EDHAS will be effectively compensated by improvement of energy efficiency depends upon the following factors:

(1) The dehumidification capacity of the desiccant wheel.

(2) With the increase of required regeneration air temperature, the temperature of waste heat recovery must increase as well. The decreasing extent of available waste heat should be quantified in order to evaluate EDHAS' performance.

(3) Desiccant dehumidification makes it possible to use chilled water of higher temperature for sensible cooling only. The degree of improvement of a chiller's cooling capacity with the increasing temperature (while keeping cooling water temperature constant) should also be determined.

In order to explore the feasibility of integrating an engine-driven chiller with desiccant dehumidification and the feasibility of providing more economically attractive alternatives for end-users, a series of research has been conducted in Tongji University, Shanghai, China. An engine-driven AC system incorporating desiccant dehumidification was configured and experimentally tested. Some critical performance data of this hybrid system, including desiccant wheel capacity, chilling COP improvement with higher chilled water temperature and waste heat recovered at different supply water temperature, were experimentally determined. The energy consumption and resulting operation cost were calculated on the basis of measured data.

2 Experimental facilities and diagnostic systems

2.1 Engine-driven chiller

Shown in Fig. 1 is the engine-driven chiller including waste heat recovery. A commercially available VC chiller with a 4FV-7 reciprocal compressor of four cylinders was selected. An automotive-derivative petroleum engine with a 32.5 kW maximum output was converted to a natural gas engine to replace the electric motor. The carburetor was replaced by a proportional mixer of equal vacuum to intake natural gas and air simultaneously. In order to precisely control the throttle open degree (therefore the flow rate of gas-air mixture), a leverage system driven by a stepping motor was developed [6]. The gas supply pressure was controlled so that lean-burn condition could be realized. The residual O_2 content in exhaust gas was always maintained above 4% to ensure complete combustion and acceptable CO/NO emissions. The gear box of the engine was always set to 1∶2 (e.g. the engine 2800 r/min, the compressor 1400 r/min) to ensure a higher efficiency of the engine. In addition, a torque rotational speed sensor was coupled in line with the shaft to measure the rotational speed and the torque transferred to the compressor. All rotational speeds in the following context were defined in terms of the compressor (rather than the engine). The maximum allowable rotational speed of the compressor was 1450 r/min while the minimum rotational speed to keep the compressor function was experimentally determined to be 700 r/min [6]. The experimental measurement interval was set at 100 r/min. Two water tanks, one for

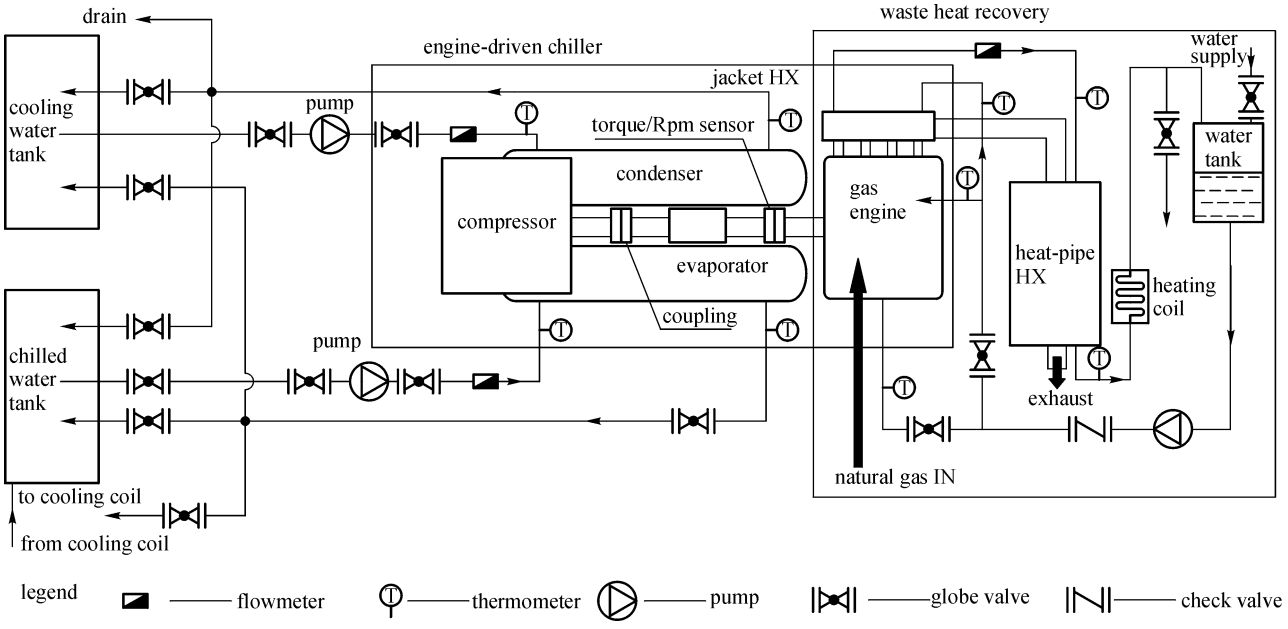

Fig. 1 Engine-driven chiller system (including waste heat recovery)

chilled water and the other for cooling water, were built to avoid using a cooling tower.

2.2 Waste-heat recovery system

The efficiency of waste heat recovery is a crucial part in hybrid AC systems. For an engine cooling system, the coolant (water) was pumped into the engine-jacket, and a two-stage waste heat recovery system was designed to ensure the recovery efficiency of exhaust heat as shown in Fig. 1. The original exhaust manifold was taken off and a jacket-type HX was installed at the first stage. Exhaust gas entered the first stage HX at ca. 500°C and left at 300°C. The second stage was a heat-pipe HX. To recover the heat from exhaust gas more efficiently, the water from the engine-cooling system entered the jacket-type HX and the heat-pipe HX in sequence. Finally, the flue gas temperature was reduced to ca. 120°C [7].

2.3 Desiccant wheel system

Figure 2 is an EDHAS incorporating an enthalpy wheel and a desiccant wheel. Both wheels use LiCl (because its regeneration temperature is 70°C and it is much easier to generate 80°C hot water used for regeneration from engine waste heat) as desiccant and the only difference is the rotational speed. For the desiccant wheel (the upper one), the rotational speed is 20 r/h; and for the enthalpy wheel (the lower one), it is 10 r/min. Fresh air passes through the pre-cooler, the enthalpy wheel, the desiccant wheel, the cooler in turn, and then is delivered to the room after being mixed with the return air. Regeneration air first exchanges enthalpy with fresh air, and then passes through the desiccant wheel after being heated. The purpose of such a compact design is to make it possible to measure the dehumidification capacity of the desiccant wheel and the efficiency of the enthalpy wheel in one set of experimental facility. When the enthalpy wheel stops, the performance of the desiccant wheel can be measured independently.

According to Ref. [8], a diagnostic system consisting of 7 sets of dry/wet bulb thermometers was built (Fig. 2), and all the thermometers were of Pt-100A type and calibrated to $+/-0.1$°C by repeatedly referring to the mercury thermometer.

Moisture mass balance ratio (MMBR) is defined as the ratio of decreasing mass of moisture in the processed air side to the increasing mass of moisture in the regeneration air side [8]. Only when MMBR falls between 0.95–1.05 can a test for dehumidification capacity be considered accurate and reliable enough. This recommended range may change with different measurement environment, but it should be taken as a criterion for judging the reasonability of the measurement system. If MMBR is smaller than 0.95 or greater than 1.05, there remain some imperfections in related equipments, which should be improved.

3 Experimental results

3.1 Dehumidification capacity: prediction vs measurement

There are many numeric models [9–13] with regard to dehumidification capacity prediction. A numeric model which solved non-linear equations by iterative method was previously set to predict the dehumidification capacity of LiCl desiccant wheel [14]. In order to determine its validity, a series of experiments was conducted to measure the dehumidification performance. The measured values of air flow rates, dry-bulb temperatures, humidity ratios of process air and regeneration air were input into the numeric model to calculate the exiting parameters. Table 1 is a comparison between some of the predicted values (in the bracket) and measured values. The measurement system can be considered reasonable.

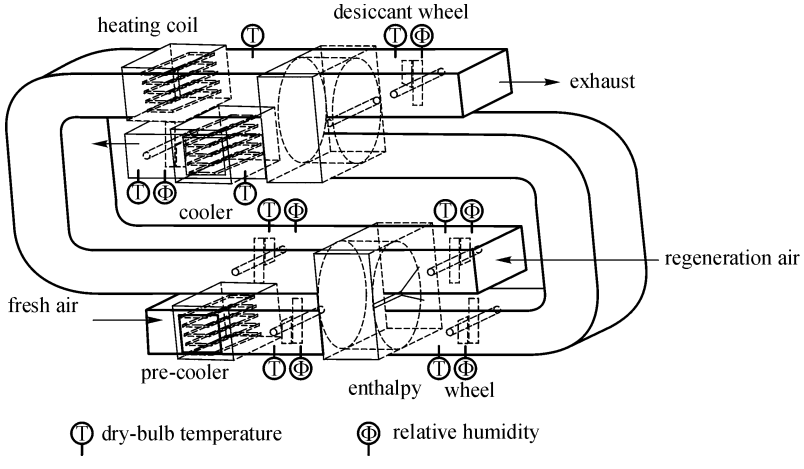

Fig. 2 Illustration sketch of humidity measurement

Table 1 Dehumidification capacity comparison: measured vs. predicted

No.	inlet parameters				outlet parameters				flow rates/($m^3 \cdot h^{-1}$)		MMBR/%
	Pro. side		Reg. side		Pro. side		Reg. side		Pro. side	Reg. side	
	T/°C	Y/($g \cdot kg^{-1}$)	T/°C	Y/($g \cdot kg^{-1}$)	T/°C	Y/($g \cdot kg^{-1}$)	T/°C	Y/($g \cdot kg^{-1}$)			
1	32.6	15.9	69.3	18.6	49.0 (48.3)	10.7 (11.43)	NA (53.5)	23.9 (23.11)	1212.6	1205.4	7.4
2	32.5	16.9	53.5	18.7	42.0 (41.5)	13.4 (14.17)	NA (43.8)	22.1 (21.66)	1208.2	1196.6	0.7
3	33.0	16.6	60.5	18.9	45.4 (44.5)	12.3 (13.21)	NA (47.6)	23.0 (22.71)	1218.4	1187.8	3.4
4	32.3	15.1	65.9	17.2	47.6 (46.3)	10.0 (11.09)	NA (49.9)	22.0 (21.77)	1123.2	1098.5	2.4
5	31.5	14.1	69.2	17.1	47.8 (46.3)	8.9 (9.98)	NA (52.4)	22.5 (21.79)	1207.9	1199.6	8.9

Because the moisture removal capacity (MRC) was very important, during the experiments the flow rates of both air streams were controlled in such a manner that the static pressure at the exit of process air was a little higher than that at the inlet of regeneration air to ensure that no regeneration air of higher humidity will leak into the process air side. Considering there was always a small amount of process air leaking into the regeneration side, the predicted results were in good agreement with the measured. On the other hand, the experiment system could be considered to be accurate enough for dehumidification measurement.

3.2 Engine performance measurement

The performance of the converted gas-engine, including shaft work (torque under variable rotational speed) and gas consumption under different chiller working conditions, was systematically measured and evaluated. At each rotational speed, the fluctuation was precisely controlled within $+/-30$ r/min. Experimental observation showed that for a given rotational speed the shaft work transferred was mainly influenced by cooling water temperature, and almost independent of chilled water temperature. The higher the cooling water temperature, the higher the torque transferred to the compressor. Because the main interest of the experiments was to determine engine energy balance, all measurements were made when cooling water temperature was kept constant at 35°C, which is the nominal operating condition specified in the national standard for chiller performance [6,7].

Table 2 lists the measured performance data of the gas-engine at variable rotational speeds.

3.3 COP changing with chilled water temperature (CWT)

According to refrigeration literature, it is possible to theoretically calculate chilling output at nominal conditions, namely chilled water 7°C–12°C and cooling water 30°C–35°C. For the engine-driven chiller developed in this paper, there is a more appropriate way to directly measure the improvement of chilling output with increasing CWT at variable rotational speeds, whose measurement procedures were as follows:

1) The rotational speed of the compressor was adjusted to nominal 1450 r/min. The flow rates of both cooling water and chilled water were so adjusted that their temperatures were maintained at $30-35 \pm 0.2$°C and $7-12 \pm 0.2$°C, respectively. Then the nominal chilling output was determined.

2) The rotational speed of the compressor was decreased while keeping the flow rates of both sides constant. Obviously, the temperature differences of cooling water and chilled water would decrease with decreasing rotational speed. The supplemented water to both water tanks were so adjusted that the temperature of chilled water exiting the

Table 2 Measured engine performance data

compressor rotational speed/($r \cdot min^{-1}$)	engine shaft work/kW	natural gas consumption/($nm^3 \cdot h^{-1}$)	engine efficiency/%
720	6.40	2.83	21.92
810	7.40	3.25	22.42
920	8.40	3.69	22.46
1020	9.70	4.02	23.81
1120	10.90	4.36	24.65
1240	12.10	4.75	25.09
1340	13.10	5.13	25.16
1420	14.00	5.28	26.16

evaporator and the temperature of cooling water exiting the condenser were maintained at 7°C and 35°C, respectively. The temperatures of the water feeding the evaporator and the condenser were recorded to determine the chilling output at decreased rotational speed. The chilling output at decreased rotational speed was calculated.

3) The CWT was increased from 7°C to 9/12/15°C in sequence. The above procedures were repeated to measure the chilling output at variable rotational speed.

Figure 3 clearly reveals the gradual increase of both chilling output (P_{co}) and COP with increasing CWT. At 1020 r/min, the measured COP is less than 4 when CWT is 7°C and increases to 5.05 when CWT increases to 15°C. At the same CWT, COP decreases with increasing rotational speed because the same condenser and evaporator handle more refrigerant and the pressure loss caused by the refrigerant intake valves increases. When CWT is at 9°C, COP at 720 r/min is 4.68 and decreases to 3.81 when rotational speed increases to 1420 r/min.

3.4 Waste heat recovery varying with supply water temperature (SWT)

When changing supply water temperature (SWT) and measuring waste heat, the level of hot water tank should be maintained constant by adjusting the two relevant valves (as shown in Fig. 1). The flow rates and temperatures of supply and return water were recorded. Then the water flow rate and SWT were kept constant and the compressor rotational speed was changed. The corresponding exit temperature was recorded to calculate reclaimed waste heat. After the performance data at all rotational speeds were recorded, the SWT was changed and measurement was repeated.

During all measurement procedures, the water supply valve was occasionally adjusted to ensure that the fluctuation of SWT did not exceed ± 0.3°C. Shown in Fig. 4 is the sum of waste heat recovered from engine cooling, jacket HX and heat-pipe HX. Apparently, the waste heat recovered from both the engine-cooling system and the exhaust decreases with increasing SWT. This is because the overall temperature difference between supply water and engine-jacket/exhaust decreases with increasing SWT. When rotational speed is 1420 r/min and SWT is 48°C, the waste heat recovered from the exhaust (13.7 kW) is slightly less than that from the engine-cooling system (14.2 kW). When SWT increases to 67°C, more waste heat could be recovered from the exhaust (12.9 kW) than from the engine-cooling system (11.6 kW). When SWT increases, the recovered heat from the engine-cooling system decreases more sharply than that from the exhaust. This observation can be readily explained by the fact that the temperature difference between supply water and engine-jacket decreases more seriously.

4 Economic benefit analysis

In order to evaluate the economic benefit of the desiccant dehumidification powered by waste heat, a hybrid system and a conventional AC system were considered for the reference building, and the energy consumption was compared.

The reference building is a small department store located in Shanghai with a floor area of 140 m^2. The staff number is 50 and latent load is 175 g/h per capita. The designed indoor air state is 25°C and 50%RH and business time is 9:00–22:00. Fresh air requirement is 30 m^3/h each person. Figure 5 is the hourly sensible load (including those from building envelop structure, internal human activity and lighting) and internal latent load (from human activity) calculated from load software.

A hybrid system, adapted from that proposed by Schmitz[1)], as shown in Fig. 6 is adopted to accommodate the above building. Part of the dehumidification task is

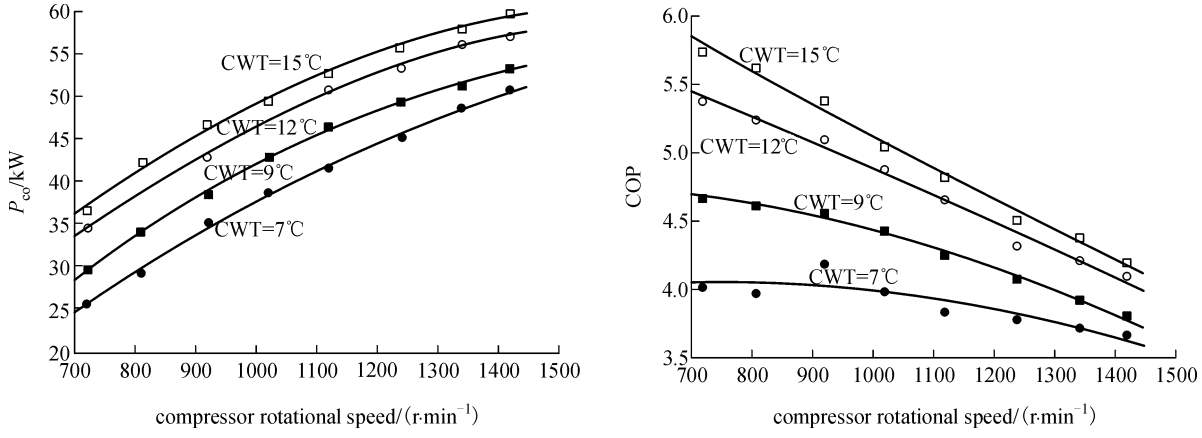

Fig. 3 Chilling output and COP changing with CWT

1) Schmitz G. A new gas driven HVAC system. Presentation at Clean Energy Conference, Shanghai, 1999

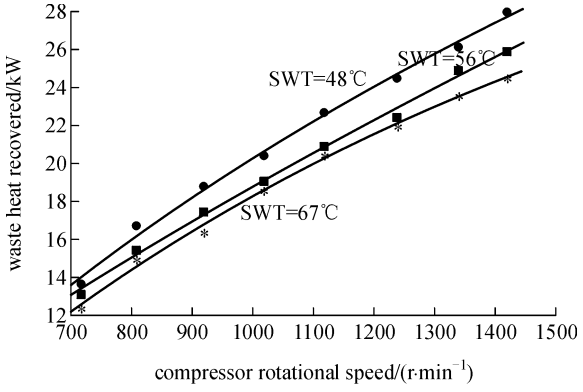

Fig. 4 Total waste heat recovered

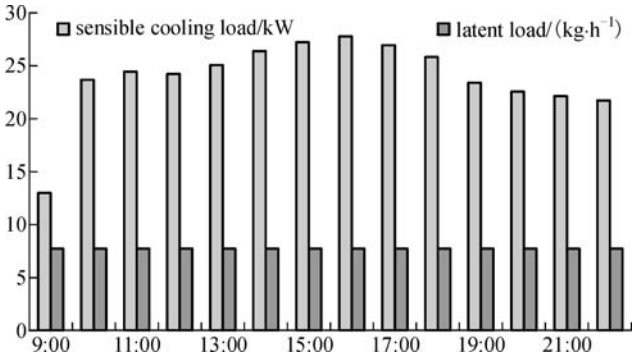

Fig. 5 Hourly sensible load and latent load of reference building within design day

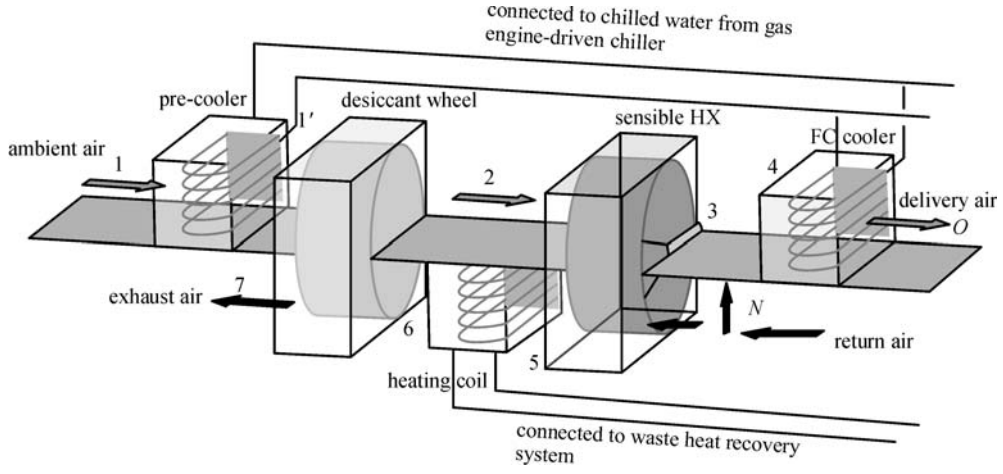

Fig. 6 Schematic illustration of hybrid system

fulfilled by pre-cooling. The ambient air (point 1) passes through the desiccant wheel to point 2, then exchanges sensible heat with the return air from the air-conditioned room (point *N*), with the return air temperature rising to point 5 and the fresh air temperature decreasing to point 3. Afterwards, the fresh air mixes with the return air (at point 4), and passes through coil HX to be cooled to supply temperature. The cooling required by the fan-coil comes from the engine-driven chiller, while the heat of the regeneration air comes from the recovered waste heat from the engine. The use of the sensible heat exchanger can effectively recover the heat from dehumidification of processed air, so that the waste heat provides only heating from point 5 to 6.

The flow rate of chilled water supplied to the pre-cooler can be adjusted according to ambient air condition, so that the condition of inlet fresh air at the desiccant wheel (point 1′) can be maintained constant at 18°C and 95%RH. In addition, the regeneration air is maintained at 70°C to achieve maximum dehumidification. The flow rates of both the fresh air and the return air are kept constant, namely no variable air volume (VAV) is considered, for the sake of simplicity.

A conventional electric VC chiller incorporating cooling dehumidification is used for comparison. The return air mixes with the fresh air and then dehumidified by a coil HX whose chilled water is supplied by an electric chiller. After the required humidity ratio is achieved (95%RH), it is reheated to a comfortable temperature. The heater is assumed to be optional and both cases (with/without heater) are calculated. Because there is no mandatory comfort requirement in China, the temperature difference for supply may be as high as 10°C if no reheating is used.

From the latent load and sensible load shown in Fig. 5, the hourly cooling and heating capacity required for the hybrid system and the conventional system (Fig. 7) were calculated. All the operational parameters, including fresh air amount (1500 m^3/h), supply air temperature, and sensible/latent load are the same for the two systems. It can be found from Fig. 7 that the cooling required is almost constant over time because the temperature difference from 9:00 to 22:00 in Shanghai is very small in summer, and the cooling capacity for the hybrid system apparently decreases due to desiccant dehumidification. Compared with those hybrid systems discussed by other researchers,

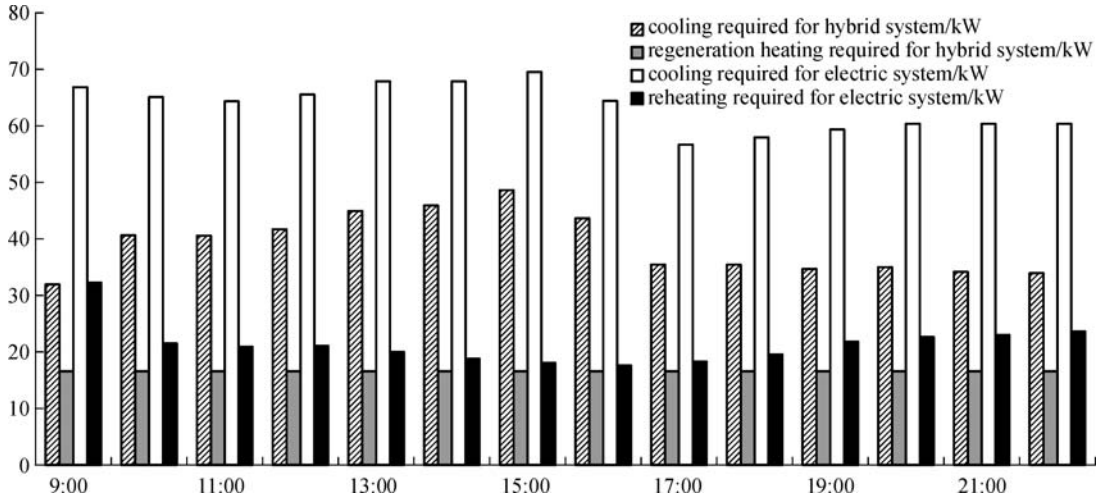

Fig. 7 Hourly cooling and heating required in hybrid AC system and conventional system

more cooling is consumed on pre-cooling due to the higher humidity ratio of ambient air.

For the hybrid system, 12°C of chilled water suffices for the dehumidification task. For the conventional AC system, 9°C of chilled water has to be used. According to the experimental data listed in Fig. 3, the compressor rotational speed can be determined to be 1120 r/min when CWT 12°C together with SWT 67°C can provide enough cooling and heat. This means both cooling and heat generated from the hybrid system are slightly higher than those required. The hourly natural gas consumption is 4.36 m^3 (standard state) per hour, the daily consumption is 56.7 m^3 (standard state). Given natural gas price is RMB 2.1 yuan per cubic meter (standard state), the daily operation cost for the hybrid system is RMB 119.2 yuan.

The COP of the electric chiller is taken as that of the engine-driven chiller measured at CWT under 1450 r/min, 3.81. The time-averaged (from 9:00 to 22:00) electricity price is RMB 0.74 yuan/kWh. For the conventional AC system, the daily operation cost is RMB 172.7 yuan if no reheating is considered (maximum supply temperature 13.7°C). If electricity is used for reheating, the daily operation cost will increase sharply to RMB 355.2 yuan.

5 Conclusions

An engine-driven chiller was combined with a desiccant wheel in this hybrid AC system. In order to evaluate the economic benefits of the system, test equipments were set up and some critical parameters were measured. For a reference building, the energy consumption within a design day was calculated for the proposed hybrid AC system and the conventional AC system. The results show that more than 40% of operation cost can be saved by integrating the engine-driven chiller with desiccant dehumidification powered by recovered waste heat. The hybrid AC system has a very promising future under present energy price conditions. The measured data of desiccant wheel and engine performance can also be useful to related researches.

Notation

AC–air-conditioning
VC–vapor-compression
COP–coefficient of performance
EDHAS–engine-driven hybrid air-conditioning system
AHU–air handing unit
HX–heat exchanger
GHP–gas heat pump
FC–fan coil
IAQ–indoor air quality
RH–relative humidity
LiCl–lithium chloride
MMBR–moisture mass balance ratio
MRC–moisture removal capacity
Pro–process air
Reg–regeneration air
CWT–chilled water temperature
SWT–supply water temperature
VAV–variable air volume

References

1. Maclaine-Cross I L. Proposal for a hybrid desiccant air-conditioning system. ASHRAE Transactions, 1988, 94(2): 1997–2009
2. Parsons B K, Pesaran A A, Bharathan D, Shelpuk B C. Improving gas-fired heat-pump capacity and performance by adding a desiccant dehumidification subsystem. ASHRAE Transactions, 1989, 95(1): 835–844
3. Zhang L Z. Energy performance of independent air dehumidification systems with energy recovery measures. Energy, 2006, 31(8/9): 1228–1242
4. Lazzarin R M, Castellotti F. A new heat pump desiccant dehumidifier for supermarket application. Energy and Building, 2007, 39(1): 59–65
5. Qin C K, Liu X. Gas-engine driven hybrid air-conditioning systems. Proceedings of Annual Meeting of China Gas Association–Application Division. Dalian, China, 2005 (in Chinese)
6. Ren J L. Research of chilling output modulation of gas-engine

driven chiller. Dissertation for the Master Degree. Shanghai: Tongji University, 2003 (in Chinese)
7. Xu Y. Waste heat recovery of gas-engine-driven chiller. Dissertation for the Master Degree. Shanghai: Tongji University, 2003 (in Chinese)
8. Qin C K, Liu X. Analysis of measurement method of dehumidification capacity of desiccant wheel. Heating-Ventilating-Air-Conditioning, 2005, 35(11): 63–66 (in Chinese)
9. Slayzak S J, Ryan J P. Desiccant Dehumidification Wheel Test Guide. National Renewable Energy Laboratory NERL/TP-550-26131, 2000
10. Barlow R S. An analysis of the adsorption process and of desiccant cooling systems: A pseudo-steady-state model for coupled heat and mass transfer. Solar Energy Research Institute Report SERI/TR-1330, Golden, Colo. 1982
11. Collier R K, Cal T S, Lavan Z. Advanced desiccant material assessment. Gas Research Institute Report GRI-86/0181, Chicago, Ill. 1986
12. Banks P J. Prediction of heat and mass regenerator performance using nonlinear analogy method: Part1–basis. Journal of Heat and Mass Transfer; ASME Transactions, 1985, 107: 222–229
13. Charoensupaya D, Worek W M. Parameter study of an open-cycle desiccant cooling system. Energy, 1988, 13(9): 739–747
14. Zheng W, Worek W M. Numerical simulation of combined heat and mass transfer processes in a rotary dehumidifier. Numerical Heat Transfer, Part A, 1993, 23(2): 211–232